

# Time Course of Tumor SUV in $^{18}\text{F}$ -FDG PET of Breast Cancer: Presentation of a Simple Model Using a Single Reference Point for Time Corrections of Tumor SUVs

Alexander R. Stahl<sup>1</sup>, Till A. Heusner<sup>2</sup>, Verena Hartung<sup>1</sup>, James Nagarajah<sup>1</sup>, Andreas Bockisch<sup>1</sup>, Steffen Hahn<sup>2</sup>, Gerald Antoch<sup>2</sup>, and Walter Jentzen<sup>1</sup>

<sup>1</sup>Department of Nuclear Medicine, University Hospital Essen, University of Duisburg-Essen, Essen, Germany; and <sup>2</sup>Department of Diagnostic and Interventional Radiology and Neuroradiology, University Hospital Essen, University of Duisburg-Essen, Essen, Germany

Tumor standardized uptake values (SUVs) vary with the interval between  $^{18}\text{F}$ -FDG injection and image acquisition. This paper presents a simple method using a single reference point to make appropriate time corrections for tumor SUVs. **Methods:** The reference point method was algebraically deduced from observations made by Beaulieu et al., who found that tumor SUVs behaved linearly over time (~30 to 75 min after  $^{18}\text{F}$ -FDG injection). Eighteen patients with breast cancer were dynamically examined with PET/CT (~60 and 80 min after  $^{18}\text{F}$ -FDG injection). Maximum SUV was calculated by applying 2 different iterative reconstruction methods (high-definition reconstruction and attenuation-weighted ordered-subsets expectation maximization). Reference points for time corrections were given, and errors for corrections obtained with the reference point method were calculated. **Results:** Variations in the reconstruction algorithm strongly influenced the coordinates of the reference point. Time corrections using the reference point method were more accurate at higher tumor SUVs (>8 at high-definition reconstruction and >6 at attenuation-weighted ordered-subsets expectation maximization) than at lower ones. **Conclusion:** A common origin of tumor SUVs over time exists in breast cancer. In combination with the linear behavior of tumor SUVs between approximately 30 and 80 min, such a reference point allows for straightforward time corrections of tumor SUVs. Parameters for image reconstruction must be considered because they influence the coordinates of the reference point.

**Key Words:** fluorodeoxyglucose (FDG); positron emission tomography (PET); standardized uptake value (SUV); exposure time; breast cancer

**J Nucl Med 2011; 52:18–23**

DOI: 10.2967/jnumed.110.077461

**U**ptake of  $^{18}\text{F}$ -FDG in malignant tumors is subject to many influencing factors. Actual uptake is determined not

only by the avidity of the tumor for  $^{18}\text{F}$ -FDG and its ability to store  $^{18}\text{F}$ -FDG but also by a variety of factors not directly relating to the tumor. Thie (1) mentioned 8 categories of confounding factors—that is, non-tumor-related factors—that influence  $^{18}\text{F}$ -FDG uptake. The interval between  $^{18}\text{F}$ -FDG injection and image acquisition (exposure time) is among the most important. The dependence of tumor standardized uptake values (SUVs) on exposure time relates to the ability of most tumors to accumulate  $^{18}\text{F}$ -FDG.

In clinical practice, uptake of  $^{18}\text{F}$ -FDG by tumors is reflected by the SUV obtained from  $^{18}\text{F}$ -FDG PET or PET/CT images. Surprisingly, there are only few references about how to correct the SUV for different exposure times to  $^{18}\text{F}$ -FDG whereas there are numerous suggestions about how to correct for other factors such as interindividual body tissue composition or different levels of blood glucose (2,3). Hamberg et al. (4) were among the first to report that  $^{18}\text{F}$ -FDG uptake in malignant tumors does not level off until several hours after injection—a feature that has since been confirmed for a variety of tumor entities (5). Wong et al. (6) proposed a power function to approximate  $^{18}\text{F}$ -FDG uptake over a limited time range. Complex methods of correcting  $^{18}\text{F}$ -FDG uptake for different exposure times have been suggested (1,6,7).

Beaulieu et al. (8) reported that SUVs in breast cancer are linear between approximately 30 and 75 min after injection. In addition, those authors gave a method by which users could correct SUVs for different exposure times to  $^{18}\text{F}$ -FDG. That method relies on data triplets that relate tumor SUVs at fixed time points after  $^{18}\text{F}$ -FDG injection to a certain slope and intercept of SUV changes over time—allowing estimation of SUVs at different time points (8). The need to correct tumor SUVs for time is of particular importance when tumor SUVs are being compared between different institutions or between baseline and follow-up (e.g., therapy monitoring).

This study is based on the findings of Beaulieu et al. (8) and their suggested correction method of tumor SUVs for different exposure times. In particular, their observation of a double linear relationship for tumor SUVs was fully adop-

Received Mar. 19, 2010; revision accepted Nov. 9, 2010.

For correspondence or reprints contact: Alexander R. Stahl, Department of Nuclear Medicine, University Hospital Essen, Hufelandstrasse 55, D-45122 Essen, Germany.

COPYRIGHT © 2011 by the Society of Nuclear Medicine, Inc.

ted for this study. The aims of this study were to simplify Beaulieu's method using a single reference point—referred to as the reference point method—and to implement this simplified method in a patient cohort with breast cancer.

## MATERIALS AND METHODS

### Time Correction According to Beaulieu

As found by Beaulieu et al. (8), there is a double (primary and secondary) linear relationship between SUVs in breast cancer and time after  $^{18}\text{F}$ -FDG injection. The primary linear relationship regards the time course of individual tumor SUVs between approximately 27 and 75 min after injection, according to:

$$\text{SUV}(t) = a_i + b_i \cdot t, \quad \text{Eq. 1}$$

with time  $t$  after  $^{18}\text{F}$ -FDG injection in units of minutes.  $a$  and  $b$  are the intercept on the SUV axis (in units of SUV) and the slope (in units of SUV/min), respectively, and differ between individual tumors as indicated by the index  $i$ . The secondary linear relationship is expressed as the dependence of the slope ( $b_i$ ) on measured SUVs at a fixed time point  $t_0$ .

$$b_i(\text{SUV}_{t_0}) = a' + b' \cdot \text{SUV}_{t_0}, \quad \text{Eq. 2}$$

with  $\text{SUV}_{t_0}$  being the measured SUV from an individual tumor at a fixed time point  $t_0$  after injection;  $a'$  (in units of SUV/min) and  $b'$  (in units of 1/min) are the intercept and slope, respectively, of this secondary linear relationship. The parameters  $a'$  and  $b'$  are dependent on the value of the fixed time point  $t_0$ .

The method of Beaulieu et al. (8) to correct for different exposure times is based on 4 exemplary secondary linear relationships (intercepts  $a'$  and slopes  $b'$ ) belonging to 4 exemplary fixed time points for SUV measurements ( $t_0 = 27, 42, 57$ , and  $71\text{--}75$  min) resulting in 4 data triplets ( $t_0, a', b'$ ). Based on any tumor SUV measured—for example, after 60 min—the user could compare the measured time point with the fixed time points  $t_0$  given by Beaulieu et al.; choose, interpolate, or extrapolate the most appropriate data triplet (i.e., the corresponding intercept  $a'$  and slope  $b'$ ); and calculate the individual slope  $b_i$  of the time course belonging to the measured SUV according to Equation 2. With this individual slope at hand, the user could calculate any tumor SUV over time based on the measured tumor SUV. The reference point method is based on the method of Beaulieu et al. to correct for time effects on tumor SUVs.

### Patients

Eighteen consecutive women with histopathologically confirmed breast cancer were examined with PET/CT. Only patients with a primary diagnosis of breast cancer before any kind of therapy were included. All patients signed an informed consent form before the injection of  $^{18}\text{F}$ -FDG. This was a retrospective study performed in accordance with the regulations of the local ethics committee and federal laws.

### Dynamic $^{18}\text{F}$ -FDG PET/CT Scans

Dynamic  $^{18}\text{F}$ -FDG PET/CT scans were obtained on a Biograph mCT (Siemens Molecular Imaging). The system consisted of a full-ring dedicated PET scanner equipped with lutetium oxyorthosilicate crystals and a  $2 \times 64$ -slice spiral CT scanner. The axial field of view of the PET detector was 21.8 cm (9).

All patients were instructed to fast 6 h before receiving an intravenous bolus injection of  $^{18}\text{F}$ -FDG (mean  $\pm$  SD,  $270 \pm 35$

MBq; range, 220–350 MBq). Patients with a blood glucose level exceeding 150 mg/dL were not included in the study. Dynamic PET imaging over 20 min was started about 60 min after  $^{18}\text{F}$ -FDG injection. A single bed position was obtained in 3-dimensional list mode covering an area from the upper thorax to the upper abdomen, with the breast tumor being in a central position. CT was acquired using low-dose technique for attenuation correction.

Dynamic, attenuation-corrected PET images were rebinned into five 4-min intervals applying a  $128 \times 128$  matrix (pixel length, 4.1 mm) and a slice thickness of 5 mm. Two different image reconstruction algorithms were applied. The first, high-definition, was based on attenuation-weighted ordered-subsets expectation maximization (OSEM) using 3 subsets and 24 iterations and additionally used a modulation of the point spread function in order to increase reconstructed spatial resolution (10). A 3-dimensional gaussian filter of 2.0 mm in full width at half maximum was applied (10). The second reconstruction algorithm was attenuation-weighted OSEM using 4 subsets with 18 iterations and a gaussian filter of 4 mm in full width at half maximum.

### Image and Data Analysis

Scans were displayed in 3 orthogonal planes (axial, coronal, and sagittal), and tumor volumes of interest were manually confined to the tumors using the view tool of the PMOD 3.0 software package (PMOD Technologies Ltd.). Maximum SUVs were calculated according to the standard formula using body weight as a surrogate for the distribution volume of  $^{18}\text{F}$ -FDG. Data were further analyzed and graphs generated with SigmaPlot 11.0 (Systat Software GmbH). In lesions smaller than 3 times the overall spatial resolution (4 mm for high-definition reconstruction, 5 mm for attenuation-weighted OSEM) within the reconstructed images, partial-volume correction was applied according to Jentzen (11) using the maximum-based recovery correction approach. For statistic comparisons, a Wilcoxon signed rank test was applied at a significance level of  $P = 0.05$ .

## RESULTS

It can algebraically be shown—as the nucleus of this work—that all individual SUV courses over time that obey the double linear relationship found by Beaulieu et al. (8) intersect at a single point when extrapolated toward smaller time points. This point of intersection, or reference point, allows for straightforward time correction of measured SUVs by the drawing of a line between the reference point and the measured SUV (Fig. 1). Only this single reference point with a time and an SUV coordinate ( $t_{\text{ref}}$  and  $\text{SUV}_{\text{ref}}$ , respectively) is necessary to make the desired time corrections. No interpolation or extrapolation is needed for the reference point method. Algebraically, any desired SUV can be calculated along the reference point method according to:

$$\text{SUV}_{\text{time desired}} = \text{SUV}_{\text{measured}} + \frac{\text{SUV}_{\text{measured}} - \text{SUV}_{\text{ref}}}{\text{time}_{\text{measured}} - t_{\text{ref}}} \times (\text{time}_{\text{desired}} - \text{time}_{\text{measured}}). \quad \text{Eq. 3}$$

The algebraic deduction of the reference point method is given in detail in the supplemental data (supplemental materials are available online only at <http://jnm.snmjournals.org>).

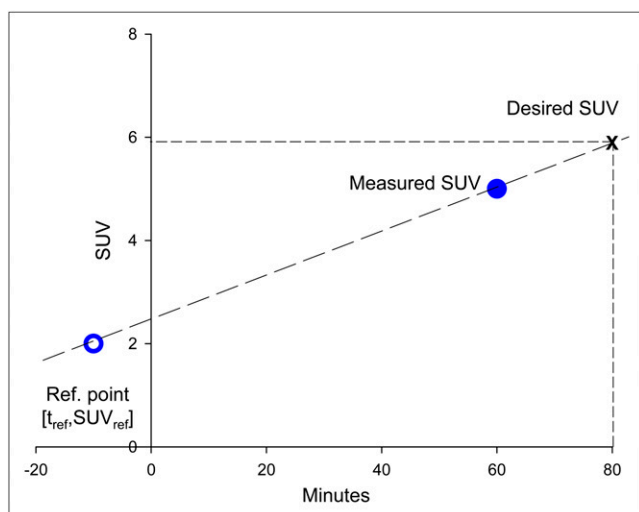


**FIGURE 1.** Illustration of reference point method for time corrections of tumor SUVs. Connect reference point (open circle with coordinates  $t_{\text{ref}}$  and  $\text{SUV}_{\text{ref}}$ ) and measured SUV (filled circle) with a line. The line represents any desired SUV at a certain time point (e.g., at the cross hair).

org). The final formulas from this algebraic deduction are for  $t_{\text{ref}}$  and  $\text{SUV}_{\text{ref}}$ :

$$t_{\text{ref}} = t_0 - \frac{1}{b'} \quad \text{Eq. 4}$$

$$\text{SUV}_{\text{ref}} = -\frac{a'}{b'}. \quad \text{Eq. 5}$$

The reference point for the application of this method can be calculated from any given dataset of SUVs that corresponds to the double linear relationship according to Beaulieu et al. (8). Table 1 contains the reference points found in this study and those calculated from Beaulieu et al. (8).

### Evaluation of Reference Point Method for Tumor SUVs in Breast Cancer

In 18 patients (mean age  $\pm$  SD,  $55 \pm 12$  y) the mean size of primary breast carcinomas was  $21 \pm 6$  mm (range, 12–36 mm). The maximum recovery coefficients applied for partial-volume correction ranged from 0.46 to 1.00. Patients were imaged from  $63 \pm 10$  to  $83 \pm 10$  min after injection. SUVs over time for individual patients and recon-

struction algorithms are given in Figure 2. As already shown for time points between about 27 and 75 min by Beaulieu et al. (8), most tumors showed an approximately linear increase in SUV; some tumors with rather low SUVs showed no increase or even a slight decrease in SUV over time.

A regression analysis of the respective individual SUV course was performed to obtain the individual intercept  $a_i$  and slope  $b_i$  (examples are shown in Fig. 2) of the primary linear relationship of tumor SUVs over time. With these data, for each patient a representative SUV at a fixed time point  $t_0 = 60$  min after injection was calculated according to Equation 1. Figure 3 plots the representative SUVs at 60 min against the rate of SUV changes ( $b_i$ ) for each patient, for the 2 different reconstruction algorithms. An underlying secondary linear relationship between SUVs at 60 min and  $b_i$  is evident ( $R^2 = 0.82$  and  $R^2 = 0.73$  for high-definition reconstruction and attenuation-weighted OSEM, respectively), as already shown by Beaulieu et al. (8). With the intercept  $a'$  and slope  $b'$  of this secondary linear relationship as well as  $t_0 = 60$  min, the reference points for both reconstruction algorithms—high-definition and attenuation-weighted OSEM—were calculated using Equations 4 and 5 (Table 1).

As a next step, we calculated the errors that occurred with the reference point method versus no correction. For this purpose, the SUVs measured at the last time point of the dynamic series were compared with SUVs measured at the first time point, that is, approximately 60 min versus 80 min and vice versa (Table 2). Figure 4 plots the absolute percentage errors for both approaches (reference point method vs. no correction) and both reconstruction algorithms. A clear advantage for reference point method correction versus no correction was seen at high SUVs (i.e.,  $>8$  for high-definition reconstruction and  $>6$  for attenuation-weighted OSEM)—that is, on average 5.8% versus 14.0% absolute error for high-definition and 4.8% versus 9.5% for attenuation-weighted OSEM ( $P < 0.01$ ), whereas at low SUVs no such advantage was seen (Fig. 4).

Finally, we examined the influence of background activity on the secondary linear relationship by subtracting mediastinal activity (maximum SUV) from tumor SUVs. With this adjustment, the secondary relationship was preserved but the grade of correlation between background-

**TABLE 1**  
Reference Points for Different Reconstruction and Analysis Approaches

Reference point	High-definition	Attenuation-weighted OSEM	High-definition – background	Attenuation-weighted OSEM – background	Beaulieu (8)
$t_{\text{ref}}$ (min) $\pm$ SEM	$5.8 \pm 6.4$	$-48 \pm 17$	$11 \pm 5$	$-42 \pm 22$	$-14$
$\text{SUV}_{\text{ref}}$ $\pm$ SEM	$5.9 \pm 1.7$	$3.2 \pm 1.6$	$2.9 \pm 1.2$	$0.67 \pm 1.2$	$3.5$

Reference points as necessary for reference point method. Time coordinate and SUV coordinate vary with different parameters for image reconstruction and methods of SUV calculation.

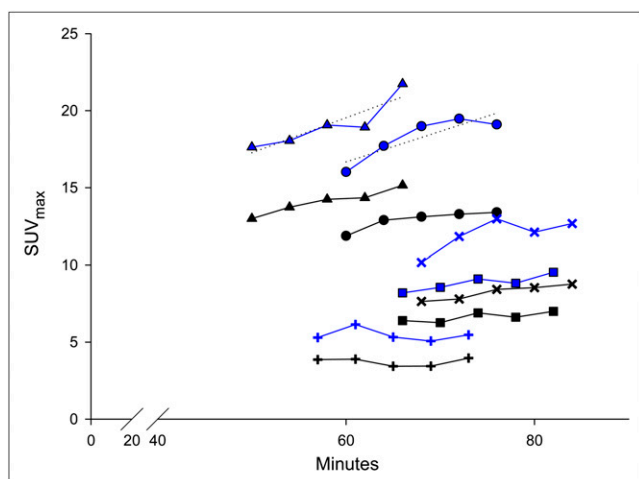


**FIGURE 2.** Maximum SUVs obtained from individual breast carcinomas over time. Two curves (same symbols) are denoted for each carcinoma, with upper curve representing high-definition reconstruction and lower curve representing attenuation-weighted OSEM. To allow for further calculation, regression lines were determined for each curve; examples are shown for the top 2 curves in the figure.

corrected SUV at 60 min and the individual slopes of the SUV time courses was not improved ( $R^2 = 0.85$  and  $R^2 = 0.67$  for high-definition reconstruction and attenuation-weighted OSEM, respectively). However, the SUV coordinates of the reference points were smaller when background correction was used (Table 1).

## DISCUSSION

The nucleus of this study was the recognition of a characteristic property of tumor SUVs in breast cancer—a property in addition to the primary linear course of tumor SUVs over time (within clinically common imaging time points)

and the secondary linear relationship between individual SUV slopes and measured tumor SUVs at fixed time points as shown by Beaulieu et al. (8). This newly found property was the existence of a common point of intersection for all primary linear SUV courses over time when they are extrapolated toward smaller time points. The existence of this common point, or reference point, was algebraically deduced from the results of Beaulieu et al. without any additional experiments. Furthermore, no information from Beaulieu et al. (8) was lost, nor was any information added.

The existence of a reference point for all individual SUV courses strongly simplifies time corrections of SUVs. Any virtual tumor SUV between about 30 and 80 min after  $^{18}\text{F}$ -FDG injection can now be calculated by the simple drawing of a line between the reference point and the measured tumor SUV (Fig. 1). Results using the reference point method for time corrections are not different from results using Beaulieu's method because both methods are algebraically equivalent. However, the reference point method avoids extrapolation or interpolation and is straightforward. Interestingly, Beaulieu has also given a single-equation method for time correction (actually it is a 2-step procedure) but without taking advantage of the simple 1-point reference lying behind his findings.

The breast cancer patient cohort investigated here served as an example for testing the reference point method. For this purpose, common PET reconstruction and SUV calculation were applied—that is, iterative reconstruction (high-definition and attenuation-weighted OSEM) and calculation of maximum SUV—and corresponding reference points according to the reference point method were calculated. Our study was not intended to confirm or refute the double linear relationship of tumor SUVs in breast cancer as found by Beaulieu et al. (8); rather, we used this information as an a priori input. Nevertheless, we also recog-

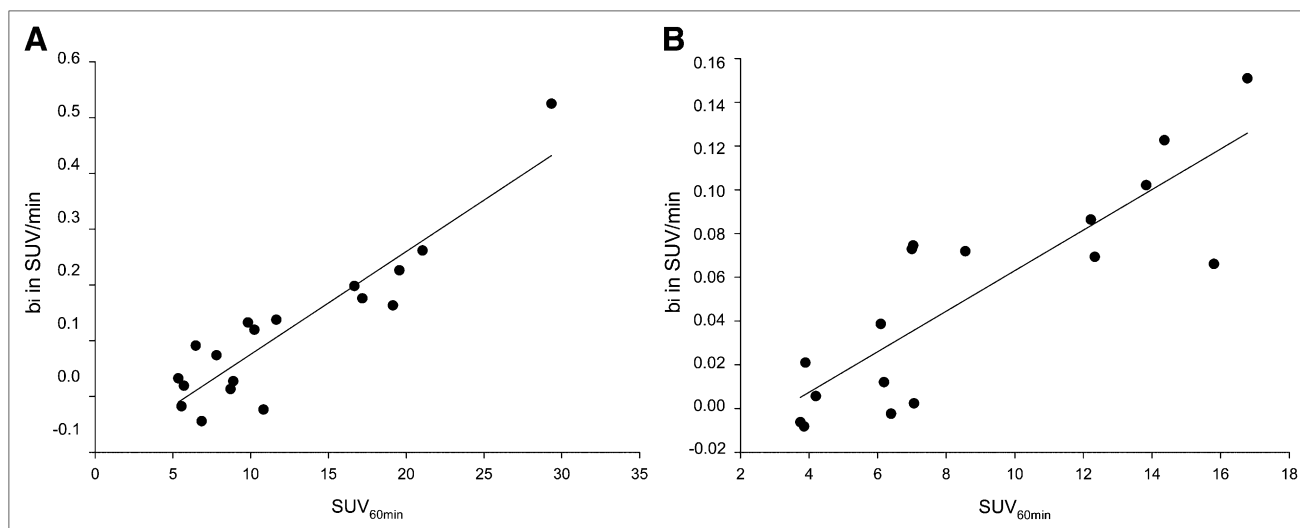


**FIGURE 3.** High-definition reconstruction (A) and attenuation-weighted OSEM (B). Shown are secondary linear relationship between SUVs at fixed time points (SUV at 60 min) and corresponding rates of change in SUV (slope  $b_i$ ). Resulting correlation had regression coefficients of  $R^2 = 0.83$  and  $R^2 = 0.72$ , respectively.

**TABLE 2**  
Errors Associated with Time Corrections

Time	High-definition		Attenuation-weighted OSEM	
	Reference point method	No correction	Reference point method	No correction
~60 to 80 min	1.2%	-9.2	1.8%	-6.0%
~80 to 60 min	-0.3%	11.2%	-0.9%	7.7%
Overall  %error	7.7% (10.8%*)	12.7%	4.5% (7.7%*)	7.3%

Percentage errors when using reference point method vs. no time correction. All differences were statistically significant at  $P \leq 0.01$  (Wilcoxon signed rank test).

\*Outer borders of 90% confidence interval for |%error| regarding uncertainty of coordinates of reference point. This border and associated |%errors| were determined using  $t_{\text{ref}} \pm 2$  SEMs and  $\text{SUV}_{\text{ref}} \pm 2$  SEMs instead of  $t_{\text{ref}}$  and  $\text{SUV}_{\text{ref}}$  for time corrections (Table 1 presents the SEMs).

nized a double linear relationship of tumor SUVs. The correlation of the secondary linear relationship was generally close ( $R^2 = 0.73$ – $0.85$ ) but somewhat lower than that found by Beaulieu et al. ( $R^2 = 0.87$ – $0.94$ ). This difference most probably stemmed from the fact that our dynamic PET protocol was shorter than that of Beaulieu et al., somewhat blurring the linear fittings of the SUV courses. As has also been observed by Beaulieu et al., time corrections of tumor SUVs were less accurate at lower SUVs than at higher ones. At low tumor SUVs, percentage measuring inaccuracies increase and interference with background carries more weight. On the other hand, the benefit from time correction decreases because changes in SUVs over time decrease at low SUVs. As a result, time corrections at low SUVs were not superior to no correction. However, one cannot rule out the possibility that the premise of a double linear relationship is biologically not fully valid at low tumor SUVs.

One might think that background subtraction from tumor SUV might improve data quality with regard to the reference

point method, particularly at low tumor SUVs, which suffer most from interfering background activity. However, we found no improvement after subtraction of background uptake, possibly because mediastinal uptake was not representative of tumor background in breast cancer and possibly because background measurements introduced an additional measuring inaccuracy into the correction algorithm.

The time and SUV coordinates of the reference point varied with the parameters applied for image reconstruction. For instance,  $\text{SUV}_{\text{ref}}$  was higher for high-definition reconstruction and lower for attenuation-weighted OSEM reconstruction. The changes in  $\text{SUV}_{\text{ref}}$  between the 2 protocols appear plausible in that high-definition reconstruction generally yielded higher SUVs than did attenuation-weighted OSEM reconstruction (Fig. 2): high-definition reconstruction has better spatial resolution than attenuation-weighted OSEM (12) and presumably higher image noise because of the higher effective iteration (3/24 vs. 4/8). Thus, any highly metabolically active inhomogeneities within the tumors or

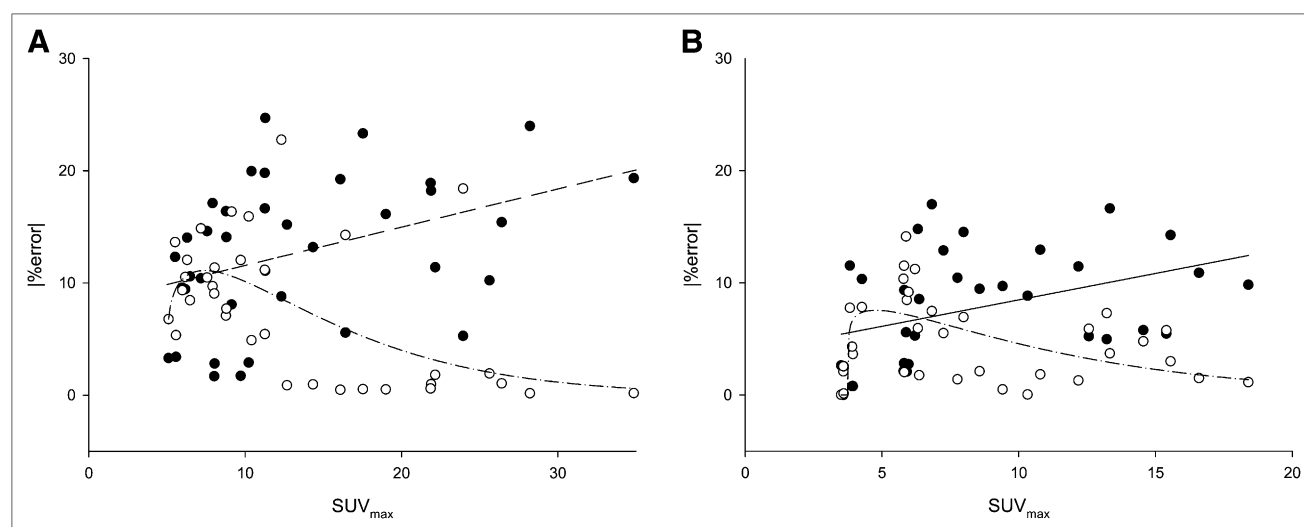


**FIGURE 4.** High-definition reconstruction (A) and attenuation-weighted OSEM (B). Percentage error (absolute values) is plotted against maximum SUV when no correction for time differences in maximum SUV was applied (●; latest vs. earliest time point and vice versa) and when time corrections according to reference point method were applied (○). Percentage errors for both methods were fitted with linear function and peak function type Weibull, respectively. Above maximum SUV of approximately 8 and 6 for high-definition reconstruction and attenuation-weighted OSEM, respectively, reference point method had clear advantage over no correction.



noise peaks would influence maximum SUV more for high-definition reconstruction than for attenuation-weighted OSEM.  $SUV_{ref}$  as calculated from Beaulieu et al. (8) using filtered backprojection for image reconstruction was comparable to attenuation-weighted OSEM (3.5 vs. 3.2, Table 1). Differences in  $t_{ref}$  occurred between protocols and also in comparison with Beaulieu et al. (8) (Table 1).

## CONCLUSION

This study found, algebraically, that the time courses of tumor SUVs in breast cancer have a common origin. In combination with the linear behavior of tumor SUVs between approximately 30 and 80 min, such a reference point allows for straightforward time corrections of tumor SUVs. The coordinates of such a reference point are highly dependent on the approach to obtaining SUVs, including protocol-specific parameters such as the image reconstruction algorithm. In the future, tumor entities other than breast cancer should also be assessed for the presence of a double linear relationship of tumor SUVs—that is, the existence of a reference point—in order to allow for simple time corrections.

## REFERENCES

1. Thie JA. Understanding the standardized uptake value, its methods, and implications for usage. *J Nucl Med*. 2004;45:1431–1434.

2. Boellaard R, O'Doherty MJ, Weber WA, et al. FDG PET and PET/CT: EANM procedure guidelines for tumour PET imaging—version 1.0. *Eur J Nucl Med Mol Imaging*. 2010;37:181–200.
3. Stahl A, Ott K, Schwaiger M, Weber WA. Comparison of different SUV-based methods for monitoring cytotoxic therapy with FDG PET. *Eur J Nucl Med Mol Imaging*. 2004;31:1471–1478.
4. Hamberg LM, Hunter GJ, Alpert NM, Choi NC, Babich JW, Fischman AJ. The dose uptake ratio as an index of glucose metabolism: useful parameter or oversimplification? *J Nucl Med*. 1994;35:1308–1312.
5. Basu S, Kung J, Houseni M, Zhuang H, Tidmarsh GF, Alavi A. Temporal profile of fluorodeoxyglucose uptake in malignant lesions and normal organs over extended time periods in patients with lung carcinoma: implications for its utilization in assessing malignant lesions. *Q J Nucl Med Mol Imaging*. 2009;53:9–19.
6. Wong CY, Noujaim D, Fu HF, et al. Time sensitivity: a parameter reflecting tumor metabolic kinetics by variable dual-time F-18 FDG PET imaging. *Mol Imaging Biol*. 2009;11:283–290.
7. Thie JA, Hubner KF, Smith GT. Optimizing imaging time for improved performance in oncology PET studies. *Mol Imaging Biol*. 2002;4:238–244.
8. Beaulieu S, Kinahan P, Tseng J, et al. SUV varies with time after injection in  $^{18}F$ -FDG PET of breast cancer: characterization and method to adjust for time differences. *J Nucl Med*. 2003;44:1044–1050.
9. Jakoby BW, Bercier Y, Conti M, et al. Performance investigation of a time-of-flight PET/CT scanner. In: *Nuclear Science Symposium Conference Record*. Piscataway, NJ: IEEE; 2008:3738–3739.
10. Panin VY, Kehren F, Michel C, Casey M. Fully 3-D PET reconstruction with system matrix derived from point source measurements. *IEEE Trans Med Imaging*. 2006;25:907–921.
11. Jentzen W. Experimental investigation of factors affecting the absolute coefficients in iodine-124 PET lesions imaging. *Phys Med Biol*. 2010;21:2365–2398.
12. Kadmas DJ, Casey ME, Black NF, Hamill JJ, Panin VY, Conti M. Experimental comparison of lesion detectability for four fully-3D PET reconstruction schemes. *IEEE Trans Med Imaging*. 2009;28:523–534.



The Journal of  
NUCLEAR MEDICINE

## Time Course of Tumor SUV in $^{18}\text{F}$ -FDG PET of Breast Cancer: Presentation of a Simple Model Using a Single Reference Point for Time Corrections of Tumor SUVs

Alexander R. Stahl, Till A. Heusner, Verena Hartung, James Nagarajah, Andreas Bockisch, Steffen Hahn, Gerald Antoch and Walter Jentzen

*J Nucl Med.* 2011;52:18-23.

Published online: December 13, 2010.

Doi: 10.2967/jnumed.110.077461

---

This article and updated information are available at:

<http://jnm.snmjournals.org/content/52/1/18>

---

Information about reproducing figures, tables, or other portions of this article can be found online at:

<http://jnm.snmjournals.org/site/misc/permission.xhtml>

Information about subscriptions to JNM can be found at:

<http://jnm.snmjournals.org/site/subscriptions/online.xhtml>

*The Journal of Nuclear Medicine* is published monthly.  
SNMMI | Society of Nuclear Medicine and Molecular Imaging  
1850 Samuel Morse Drive, Reston, VA 20190.  
(Print ISSN: 0161-5505, Online ISSN: 2159-662X)

© Copyright 2011 SNMMI; all rights reserved.

The logo for the Society of Nuclear Medicine and Molecular Imaging (SNMMI) consists of the letters 'S', 'N', 'M', and 'I' arranged in a 2x2 grid. Each letter is white and set within a red square.  
SOCIETY OF  
NUCLEAR MEDICINE  
AND MOLECULAR IMAGING